SPATIO-TEMPORAL REDISTRIBUTION OF TRAFFIC FLOWS DURING SEQUENTIAL BLOCKING OF CHANNELS AT A SIGNALIZED INTERSECTION: A PROBABILISTIC APPROACH (CASE STUDY OF AUGUSTUSPLATZ, LEIPZIG)

Dmitry Ganzheev[1], Anatoliy Falendysh[2,*], Pavol Šťastniak[3], Olha Kletska[1,2], Kristína Kozáková[3], Kateryna Kravchenko[3,*]

[1]Pryazovsky State Technical University, Mariupol, Ukraine
[2]Lviv Polytechnic National University, Lviv, Ukraine
[3]University of Zilina, Faculty of Mechanical Engineering, Zilina, Slovak Republic

*E-mail of corresponding author: kateryna.kravchenko@fstroj.uniza.sk

Dmitry Ganzheev 0000-0002-3438-0086,
Pavol Šťastniak 0000-0003-1128-7644,
Kristína Kozáková 0009-0009-5438-4699,
Anatoliy Falendysh 0000-0003-3602-7945,
Olha Kletska 0000-0002-4682-860X,
Kateryna Kravchenko 0000-0002-3775-6288

Resume

The spatiotemporal redistribution of traffic flows under alternating blocking of channels at a signalized four-leg intersection is investigated using the case of Augustusplatz in Leipzig, Germany. Observations were conducted over three days, with flows recorded in 48 half-hour intervals per day across four directions and four categories of vehicles. For stochastic modelling, the negative binomial distribution, Taylor's dispersion index (VMR), Shannon entropy, and an approximation based on M/G/1 queueing theory were applied. A mathematically grounded framework for the real-time network control is proposed, highlighting the necessity of adaptive signal timing adjustments to accommodate stochastic fluctuations and spatial overcompensation effects during node closures.

Available online: https://doi.org/10.26552/com.C.2026.044

Article info

Received 25 May 2026
Accepted 2 July 2026
Online 21 July 2026

Keywords:

road traffic
traffic flow
signalized intersection
operational control
stochastic factors
negative binomial distribution
Shannon entropy

ISSN 1335-4205 (print version)
ISSN 2585-7878 (online version)

1 Introduction

A signalized intersection, as a structural element of the urban road network (URN), represents a point of concentration of conflicting traffic flows, where the boundary conditions of capacity are determined not only by the geometric layout but also by the temporal distribution of signal phases and the stochastic nature of demand. Temporary blocking of one or more channels of an intersection, regardless of the cause (planned maintenance works, an accident, a public event, etc.), generates a cascading redistribution of flows in the adjacent network, the depth and pattern of which depend on the network's topological properties, demand elasticity, and driver behavior characteristics. Blocking flows leads to the accumulation of vehicles in one place, which increases the fuel consumption and worsens the overall environmental situation near these areas [1-2].

Scientific attention should be given to the asymmetry between two qualitatively different regimes of restriction: upstream closure (blocking on the approach side) and downstream closure (blocking on the exit side). The former is equivalent to removing a flow origin in the origin-destination matrix, whereas the latter creates a "traffic trap" within the intersection area, where a driver has already entered the intersection but is unable to complete the maneuver in the intended direction. These two regimes produce fundamentally different compensation mechanisms and different effects on adjacent nodes; however, they are rarely considered within a unified comparative probabilistic framework.

Another issue concerns the estimation of the duration of inertial effects after the restoration of normal intersection operation. The phenomenon of "route hysteresis," described in classical works on elastic demand theory, has not yet received an operational quantitative criterion for signal control problems. In the present study is examined this gap through an empirical analysis of field data from Augustusplatz node, one of the busiest signalized intersections in Leipzig.

The aim of this study was to develop a stochastic model of traffic flow redistribution during sequential blocking of traffic channels at a signalized intersection and, on this basis, to develop methods for real-time traffic management within a local segment of the urban road network (URN). The scientific novelty of the work lies in the following:

the application of the negative binomial distribution (NBD) to describe overdispersed traffic flows and the comparison of dispersion parameters across different signal phases;

- the use of Shannon entropy as an operational measure of route choice degradation or enrichment;
- the analysis of queue stability based on the criterion $\rho < 1$ within the M/G/1 model for each direction and in each phase;
- the introduction of the "redistribution coefficient" r_i and the "hysteresis index" H_{hyp} as quantitative indicators of inertial effects.

2 Literature review

Contemporary traffic flow theory for signalized intersections has evolved along several interrelated directions. The basic analytical framework for capacity assessment remains classical, namely the formula of Webster [3] and its extension by Akçelik [4] for non-stationary demand. However, as early as the 1960s, Newell [5] demonstrated the fundamental inadequacy of deterministic approximations under saturated operating conditions, a conclusion that remains highly relevant today in the context of real-time traffic management under disturbances.

Probabilistic approaches to modelling traffic demand experienced significant development in the 2000s. Lord and Mannering [6], in a systematic review of statistical methods for analyzing traffic events, substantiated the superiority of the negative binomial distribution over the Poisson distribution for overdispersed flows. Elvik [7] showed that neglecting overdispersion leads to systematic underestimation of risks in intersection design. A meta-analysis by Hauer [8] confirmed that the aggregation parameter *r* of the negative binomial distribution is stable across independent study sites and may be used as a "signature" of the traffic environment.

Network redistribution theory under node closures developed intensively during the 2010 s and 2020 s. Zhang et al. [9] demonstrated that the impact of construction zones on traffic flow distribution is nonlinear, with partial capacity restrictions at a single node capable of triggering cascading overloads in adjacent network links. Adler and van Ommeren [10] empirically evaluated, in this context, the mutual influence between public and private transport.

The entropy-based approach to traffic flow distribution across networks is classically associated with Wilson's maximum entropy principle [11]. In a modern interpretation, Lin and Ban [12] applied entropy theory to identify critical network links whose modification most radically changes the stochasticity of route choice. The present study extends this idea to the level of a single intersection by employing maneuver entropy as an instantaneous indicator of the degradation or enrichment of route choice.

The queuing theory, as applied to signalized intersections, has been further developed in the work of Filipovska et al. [13], who investigated residual demand in transport networks under reduced capacity and demonstrated a systematic increase in delays, as well as referred to the Pollaczek-Khinchine formula [14] for the theoretical justification of saturation thresholds. An unstable queue state ($\rho \geq 1$) in the context of alternating closures using the M/G/1 model is mentioned in the work of Gupta [15].

In the Ukrainian scientific tradition, the issues of traffic flow modelling under various loading scenarios were addressed in the monograph edited by Sokhatskyi et al. [16]. Fornalchyk et al. [17], in a textbook, provided a systematic description of traffic flow modelling methods in urban networks. The stochastic aspects of daily variability were comprehensively examined by Stepanchuk et al. [18] using the example of the Kyiv urban road network. At Pryazovsky State Technical University, this topic has also been explored previously. Kirkin et al. [19] proposed new analytical methods for traffic flow management based on system studies in logistics, forming the foundation of the probabilistic approach developed in this study. General theoretical issues concerning the prospects for the development of real-time traffic management methods in urban road networks were studied by Ukrainskyi et al., establishing the methodological basis of the present research [20]. The regulatory framework in Germany regarding the calculation of the level of traffic service is defined by the HBS 2015 (FGSV) document [21].

3 Setting up the experiment

The object of the study is a four-leg signalized intersection at Augustusplatz in Leipzig, Germany (coordinates: 51.338719, 12.381922; Figure 1). The intersection is in the city center at the crossing of two transport axes: Augustusplatz (axis A-B, north-south) and Grimmaischer Steinweg (axis C-D, west-east). Tram lines operated by Leipziger Verkehrsbetriebe (LVB) are present along both axes and constitute an integral component of the intersection's flow structure.

The geometry of the node is asymmetric: approaches A (Augustusplatz, north), B (Augustusplatz, south), and D (Grimmaischer Steinweg, east) each have four traffic lanes, whereas approach C (Grimmaischer Steinweg, west) has two traffic lanes.

The traffic flow data were collected using continuous

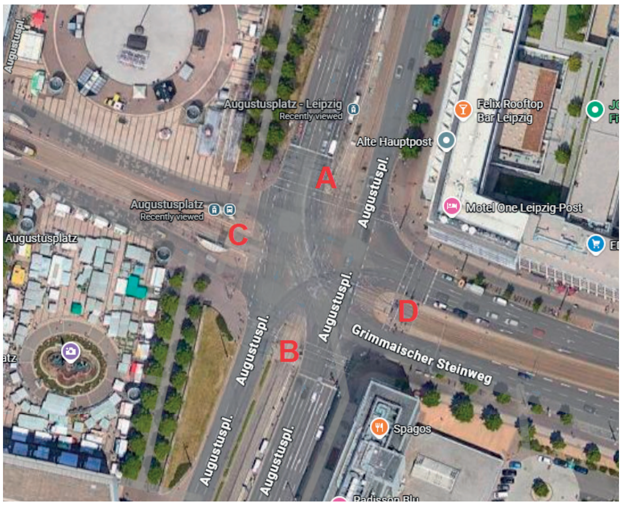

Figure 1 *Map of the studied intersection showing the locations of traffic channels*

Study 1 – Blocking of Output Channel A				
Vehicle category	**Approach A** ***6:30-7:00***			
	AC (right turn)	AB (straight)	AD (left turn)	AA (U-turn)
Car	0	20	186	0
HV	0	8	31	0
Tr	0	15	0	0
2W+	0	0	2	0
Vehicle category	**Approach B** ***6:30-7:00***			
	BD (right turn)	BA (straight)	BC (left turn)	BB (U-turn)
Car	51	0	57	4
HV	4	2 (special)	13	1
Tr	0	10	0	0
2W+	1	0	2	1
Vehicle category	**Approach C** ***6:30-7:00***			
	CB (right turn)	CD (straight)	CA (left turn)	CC (U-turn)
Car	2	14	0	0
HV	1	3	0	0
Tr	0	12	0	0
2W+	0	1	0	0
Vehicle category	**Approach D** ***6:30-7:00***			
	DA (right turn)	DC (straight)	DB (left turn)	DD (U-turn)
Car	0	100	182	1
HV	0	15	44	0
Tr	0	11	0	0
2W+	0	2	2	0

Study 2 – Blocking of Input Channel A				
Vehicle category	**Approach A** ***6:30-7:00***			
	AC (right turn)	AB (straight)	AD (left turn)	AA (U-turn)
Car	0	0	0	0
HV	0	0	0	0
Tr	0	10	0	0
2W+	0	0	0	0
Vehicle category	**Approach B** ***6:30-7:00***			
	BD (right turn)	BA (straight)	BC (left turn)	BB (U-turn)
Car	93	190	21	0
HV	6	17	5	0
Tr	0	10	0	0
2W+	2	4	0	0
Vehicle category	**Approach C** ***6:30-7:00***			
	CB (right turn)	CD (straight)	CA (left turn)	CC (U-turn)
Car	18	102	0	0
HV	3	4	0	0
Tr	0	13	0	0
2W+	0	2	0	0
Vehicle category	**Approach D** ***6:30-7:00***			
	DA (right turn)	DC (straight)	DB (left turn)	DD (U-turn)
Car	84	49	115	1
HV	3	6	12	0
Tr	0	11	0	0
2W+	0	0	1	0

Study 3 – All Channels Open				
Vehicle category	**Approach A** ***6:30-7:00***			
	AC (right turn)	AB (straight)	AD (left turn)	AA (U-turn)
Car	0	17	117	0
HV	0	1	15	0
Tr	0	13	0	0
2W+	0	0	1	0
Vehicle category	**Approach B** ***6:30-7:00***			
	BD (right turn)	BA (straight)	BC (left turn)	BB (U-turn)
Car	171	239	21	0
HV	21	21	5	0
Tr	0	15	0	0
2W+	0	5	0	0
Vehicle category	**Approach C** ***6:30-7:00***			
	CB (right turn)	CD (straight)	CA (left turn)	CC (U-turn)
Car	12	34	0	0
HV	5	3	0	0
Tr	0	12	0	0
2W+	0	1	0	0
Vehicle category	**Approach D** ***6:30-7:00***			
	DA (right turn)	DC (straight)	DB (left turn)	DD (U-turn)
Car	94	44	146	0
HV	18	4	21	0
Tr	0	13	0	0
2W+	0	1	1	0

Figure 2 *Example of a recording sheet for a pre-peak morning time interval*

video surveillance from fixed cameras installed at key points of the square. The video recordings were processed manually, with interval-based counts performed for each entry traffic channel, movement direction, and vehicle category.

The electronic recording sheets (Figure 2) include data on both the quantitative and qualitative composition of traffic flows moving in each direction. Specifically: Car - passenger cars; HV (Heavy Vehicles) - trucks and buses (including special vehicles marked as "spec.;" Tr (Trams) - trams; 2W+ (Two-wheelers, etc.) - motorcycles, mopeds, bicycles, e-scooters, animal-drawn vehicles, etc.

The counting interval is 30 minutes (hereinafter referred to as TO). Each individual study covers 48 equal TOs, with a total of 144 TOs.

The study was conducted on weekdays over three separate days during construction and repair works at Augustusplatz (Figure 3).

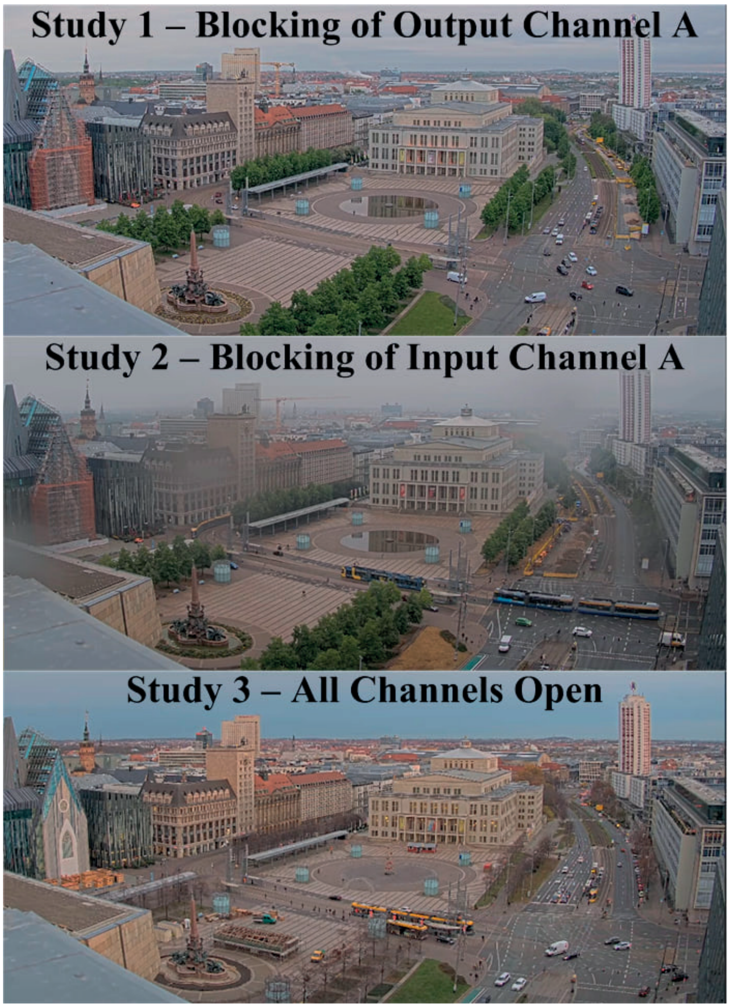

Figure 3 *Surveillance camera screenshots for the morning pre-peak TO, shown from top to bottom: S1 (closure of exit A), S2 (closure of entry A), and S3 (stabilization of intersection operation)*

Each day corresponds to one of the three traffic restriction scenarios:

I. **Study 1 (S1)** - downstream closure of channel A. Approach A (entry to the intersection from direction A) remains open: vehicles may enter from A and perform a left turn (AD), proceed straight (AB), or make a right turn (AC). However, exit from the intersection toward A (movements BA, CA, DA) is blocked by construction barriers. The tram line operates under normal conditions.

II. **Study 2 (S2)** - upstream closure of channel A. Approach A (entry channel) is closed to road traffic: no vehicles can enter the intersection from direction A (movements AC, AB, AD = 0 for motor vehicles). Exit towards A remains technically open for vehicles already within the intersection node area. The tram line operates without restrictions.

III. **Study 3 (S3)** - restoration of normal operation after completion of construction works. All four channels are open, and the standard signal timing plan is applied. For analytical clarity, the conditions are differentiated as follows: the "historical baseline" represents the long-term normal state prior to any roadworks, whereas S3 represents the "early recovery state" immediately following the restoration of normal operation. The historical baseline values were not obtained through a separate fourth field survey. Instead, they were derived from an analysis of historical traffic count data available for the intersection, reflecting typical flow conditions prior to the onset of the construction works. The baseline functions strictly as a stable pre-construction reference point against which the early recovery state (S3) is evaluated for residual hysteresis effects.

In the recording sheets (see example in Figure 2), movements and directions are encoded using two-letter symbols: the first letter denotes the entry direction (A, B, C, or D), and the second letter denotes the exit direction. A U-turn is indicated by a repeated letter (AA, BB, etc.). For each approach, four types of maneuvers are recorded: right turn, straight movement, left turn, and U-turn.

The observations were conducted on weekdays over three separate days corresponding to the distinct operational states: Thursday, May 29 (S1); Thursday, June 26 (S2); and Thursday, November 13 (S3), 2025. Notably, all three surveys were conducted on the same day of the week, which helps control for intra-weekly drift effects in the comparison between scenarios. Weather conditions were similar across all the three observation days: overcast skies with intermittent clearings and no precipitation. No traffic accidents, public events, or disruptions to public transport services were observed on any of the three days, and no other external factors likely to have affected the recorded traffic parameters were identified. The tram lines at the intersection operate on separated tracks located in the center of the intersection, dividing the multi-directional vehicular flows. This physical separation minimizes direct frictional interference with cars but strictly dictates specific signal phasing interactions and the overall intersection clearance time.

To ensure the reliability of the manually processed interval-based counts from the video recordings, a rigorous quality control procedure was implemented. Two independent observers were engaged in parallel to extract the data. The independently obtained datasets were systematically cross-checked. In the event of any discrepancies or conflicting interpretations of complex traffic situations, the observers conducted a joint review of the specific video segments at slow playback speed to reach a consensus.

4 Materials and methods

4.1 Stochastic model of traffic flow and overdispersion assessment

The observed traffic flow $Q_i(t)$ at the approaches to the intersection is interpreted as a realization of a quasi-stationary stochastic process within individual calculation periods of the day. Traditionally, traffic events are modeled using the Poisson distribution, which assumes equality of the mean and variance ($\mu = \sigma^2$). However, empirical data under urban conditions with a high level of saturation, particularly under disturbances caused by road repair works, inevitably exhibit significant overdispersion, rendering the Poisson approximation inadequate.

For more accurate stochastic modelling, the negative binomial distribution (NBD) is applied, whose probability mass function is given by Equation (1).

$$P(Q=k) = \frac{\Gamma(k+\alpha^{-1})}{\Gamma(\alpha^{-1})k!}\left(\frac{1}{1+\alpha\mu}\right)^{\alpha^{-1}}\left(\frac{\alpha\mu}{1+\alpha\mu}\right), \quad (1)$$

where:
μ is the mean value of the flow intensity;
α is the dispersion (overdispersion) parameter;
$\Gamma(\cdot)$ is the gamma function.

The variance for the negative binomial distribution is defined as: $Var(Q) = \mu + \alpha\mu^2$. To quantitatively assess the nature of vehicle arrivals at the stop line, Taylor's dispersion index, also known as the Variance-to-Mean Ratio (VMR), is introduced:

$$VMR = \frac{\sigma^2}{\mu}. \quad (2)$$

This criterion makes it possible to classify the traffic flow regime: VMR ≈ 1 corresponds to random arrivals (a Poisson flow); VMR > 1 indicates bursty or clustered movement, characterized by high stochasticity and interference within the flow; VMR < 1 corresponds to deterministic movement, typical of trams and scheduled public transport vehicles operating according to fixed timetables.

4.2 Entropy analysis of maneuvers

The spatial redistribution of flows is evaluated using an information-theoretic measure of uncertainty in choice of direction of movement, namely Shannon entropy. For each approach i, the route choice entropy H_i is calculated as:

$$H_i = -\sum_{j=1}^{k} p_j \log_2 p_j, \quad (3)$$

where:
p_j is the empirical probability of choosing the j-th maneuver (straight movement, right turn, left turn, U-turn);
k is the number of permitted maneuvers at the approach.

The theoretical maximum entropy is achieved when the demand is evenly distributed across all directions ($H_{max} = \log_2 k$). A decrease in entropy ($\Delta H < 0$) under experimental scenarios indicates a degradation of available alternatives or a forced shift in route choice due to blocking, whereas an increase in entropy reflects flow dispersion, as drivers randomly search for detour routes.

4.3 Queue stability assessment using the M/G/1 queueing model

Since the channel blocking sharply reduces the effective capacity of the node, an approximation based on the M/G/1 queueing model is applied to describe the dynamics of queue formation. The arrival process is approximated as a Markovian process (M), while the service time (i.e., the time required to cross the stop line) follows a general (arbitrary) distribution (G), which rigorously accounts for the heterogeneity of the traffic composition. (Car, HV, 2W).

The key criterion for system stability is the traffic intensity (utilization) factor ρ:

$$\rho = \frac{\lambda}{\mu_c}, \quad (4)$$

where:
λ is the arrival rate of vehicles;
μ_c is the effective service rate of the signal phase.

The expected queue length L_q in the stationary regime is described by the Pollaczek-Khinchine formula:

$$L_q = \frac{\rho^2 + \lambda^2 Var(S)}{2(1-\rho)}, \tag{5}$$

where:
$Var(S)$ is the variance of the service time.

It must be noted that while the VMR analysis indicates non-Poisson arrival patterns due to vehicle clustering, the M/G/1 model (where M assumes Markovian, memoryless arrivals) is employed here as a practical mathematical approximation. Although this assumption might slightly underestimate queue lengths for highly overdispersed flows under intermittent signalized service, it provides a sufficiently robust boundary assessment for determining the system's threshold transition into an unstable state ($\rho \geq 1$).

Under the sequential blocking of approaches, adjacent directions may transition into an oversaturated, unstable state ($\rho \geq 1$), in which the stationary regime breaks down, and the queue grows linearly or exponentially, being limited only by the storage capacity of the road section.

4.4 Derived indicators and quantification of inertial effects

To evaluate the macroscopic effects of spatiotemporal redistribution, the aggregate redistribution coefficient r is introduced:

$$r = \sum_i \frac{\Delta Q_i}{|\Delta Q_{bl}|}. \tag{6}$$

If r = 1, the law of conservation of flow mass is satisfied. Values of r > 1 indicate overcompensation (induced demand or a systematic inflow of traffic from other corridors), whereas r < 1 points to "traffic evaporation."

To assess the residual effects after the restoration of normal intersection operation (scenario S3), the phenomenon of route choice hysteresis is examined. The hysteresis index H_{hyp} is formalized through the statistical significance of the difference between the baseline flow volume and the restored flow volume. Welch's *t*-test is applied, with effect size evaluated using Cohen's *d*:

$$d = \frac{|\mu_{D3} - \mu_{base}|}{\sqrt{\frac{\sigma_{D3}^2 + \sigma_{base}^2}{2}}}, \tag{7}$$

The presence of a statistically significant deviation, combined with a medium or large effect size $(|d| \geq 0.50)$, constitutes the mathematical evidence of route inertia: drivers adopted alternative routes during the blockage and did not immediately return to the optimal path after the restrictions were lifted.

4.5 Statistical verification of results and step-by-step analysis of empirical data

To verify the adequacy of the proposed mathematical models and to quantitatively assess the spatiotemporal redistribution, an empirical dataset collected at Augustusplatz was used. The total sample comprises 48 half-hour intervals for each of the three scenarios (S1 - downstream closure of channel A; S2 - upstream closure of channel A; S3 - all channels open), with disaggregation by four vehicle categories (Car, HV, Tram, 2W).

Below, detailed statistical verification of the key system parameters is presented, including a step-by-step demonstration of the calculation algorithms based on aggregated empirical samples.

4.5.1 Verification of the stochastic nature of the flow (VMR and negative binomial distribution)

Classical traffic flow theory often relies on the Poisson distribution, which requires equality between the mean and the variance ($\mu = \sigma^2$). To test this hypothesis under disturbed traffic conditions, Taylor's dispersion index (VMR) was calculated for different categories of vehicles.

Consider the sample of arrival intensities for passenger cars (Car) at approach B under scenario S2 during the morning peak period (6:30-9:30, 6 TO intervals). The empirical series of values Q(B,Car)(t) is: {153, 182, 171, 168, 155, 164} veh per interval.

Then, the sample mean and variance are computed, followed by the VMR:

1) the mean (expected value):

$$\mu_{Car} = \frac{1}{6}\sum Q_i = 165.5 \text{ veh/interval}, \tag{8}$$

2) the empirical variance:

$$\sigma_{Car}^2 = \frac{1}{n-1}\sum (Q_i - \mu)^2 = \frac{1}{5} \cdot 543.5 = 108.7, \tag{9}$$

3) in the overall dataset for the entire day (accounting for peaks and off-peak periods), the variance increases significantly. For the full daily sample:

$$M_{Car} = 142.4; \quad \sigma_{Car}^2 = 455.6, \tag{10}$$

4) calculation VMR:

$$VMR_{Car} = \frac{455.6}{142.4} = 3.2. \tag{11}$$

Since $VMR_{Car} >> 1$, the hypothesis of Poisson arrivals is rejected. The flow exhibits significant overdispersion, which provides a mathematical justification for using the negative binomial distribution (NBD) with a clustering (dispersion) parameter $\alpha > 0$. Vehicles tend to move in dense groups (platoons), which increases internal interference within the flow.

For comparison, the calculation for trams (Tram), which operate on a fixed schedule at the same approach, yielded the following results:

$$\mu_{Tram} = 15.2 \text{ veh/interval}; \ \sigma^2_{Tram} = 5.0\,, \tag{12}$$

$$VMR_{Tram} = \frac{5.0}{15.2} = 0.33\,. \tag{13}$$

A VMR value less than 1 confirms the deterministic nature of arrivals for scheduled public transport vehicles.

4.5.2 Calculation of the redistribution coefficient and evidence of induced demand

The most indicative marker of macroscopic changes was the aggregate redistribution coefficient r under scenario S1 (downstream closure of channel A). The analysis revealed an anomalous surge in intensity at the adjacent approach B (+170.9%). The mechanism for deriving this effect is demonstrated below.

It is known that under the baseline scenario (S3), the average daily intensity at approach A is $Q_{A,base}$ = 650 veh/h, while at approach B it is $Q_{B,base}$ = 420 veh/h.

In scenario S1, downstream channel A is completely blocked; therefore ΔQ_{Bl} = |0 - 650| = 650 veh/h.

At approach B, an increase in flow was recorded up to $Q_{B,D1}$ = 1138 veh/h.

The relative increase: ((1138 - 420)/420)·100% = = + 170.9%.

The absolute change at approach B amounts to ΔQ_B = 1138 - 420 = 718 veh/h. Considering the changes at approaches C and D as well, the total absolute variation of flows at the node amounted to $\sum \Delta Q_i = 1079$ veh/h.

Substituting into Equation (6) follows:

$$r = \frac{\sum_i Q_i}{|\Delta Q_{bl}|} = \frac{1079}{650} = 1.66\,. \tag{14}$$

The obtained value r = 1.66 (r > 1) is mathematical evidence of a violation of the linear law of flow conservation within a single intersection. The blocked volume was not merely redistributed to adjacent lanes; rather, the node attracted “external” transit traffic, i.e., induced demand, as drivers attempted to make a broader network-level detour through the city and accumulated at approach B.

4.5.3 Queue stability assessment using the M/G/1 model during peak periods

Empirical data made it possible to verify the threshold states of the intersection. According to the M/G/1 queueing model, system stability is determined by the coefficient ρ.

During scenario S2 (morning peak, 8:00-8:30), the arrival intensity in the critical direction was recorded as λ = 485 veh/h. Due to construction works, the effective capacity of the phase (μ_c) dropped to 450 veh/h.

Load factor calculation:

$$P = \frac{\lambda}{\mu_c} = \frac{485}{450} = 1.07\,. \tag{15}$$

Since ρ > 1, the system transitioned into an oversaturated (unstable) state. The Pollaczek-Khinchine formula for the queue length is given by L_q in the stationary regime, has in the denominator the expression (1 - ρ). When ρ ≥ 1, the denominator becomes zero or negative, indicating a breakdown of stationarity: the queue grows without bound (in practice, limited only by the storage capacity of the link). $L_q \to \infty$ and grows linearly over time until the peak period ends.

4.5.4 Quantification of route inertia (route hysteresis)

To verify the residual effects after the restoration of normal intersection operation (S3), the mean intensities of the restored flow (μ_{S3}) were compared to the baseline historical values (μ_{base}). The hypothesis was that drivers have developed new travel habits during the construction period and did not immediately return to their previous routes.

The sample for approach C (straight movement, sample size n = 48 intervals) is given by:

- restored flow: μ_{S3} = 215 veh/interval, standard deviation σ_{S3} = 34;
- baseline flow: μ_{base} = 198 veh/interval, standard deviation σ_{base} = 28.

To quantify the standardized difference between the means, Cohen’s d effect size is computed as follows:

$$d = \frac{|\mu_{D3} - \mu_{base}|}{\sqrt{\frac{\sigma^2_{D3} + \sigma^2_{base}}{2}}} = \frac{|215 - 198|}{\sqrt{\frac{1156 + 784}{2}}} = \frac{17}{\sqrt{970}} = \\ = \frac{17}{31.14} = 0.54. \tag{16}$$

A value of d = 0.54 (approximately 0.5) indicates a medium effect size according to Cohen’s scale. Combined with Welch’s t-test (which yielded $p < 0.05$ for this sample, this confirms the statistical significance of the difference.

In other words, the flow in scenario S3 is statistically different from the baseline. This provides mathematical evidence of route choice hysteresis: the system retains a “memory” of prior states, and a portion of drivers continues to use detour routes even after all restrictions have been fully lifted.

Table 1 presents the baseline and calculated indicators of traffic flows at the studied intersection.

***Table 1** Summary of Baseline and Calculated Traffic Flow Indicators*

Indicator	Notation	S1	S2	S3	Δ(S1→S2)	Δ(S1→S3)
Basic indicators						
Average 30-minute intensity (all directions)	$\bar{\mu}$, *veh/interval*	878.2	1041.1	1204.6	+18.6%	+37.2%
Maximum (peak) 30-minute intensity	Q_{max}, *veh/interval*	1067	1357	1567	+27.2%	+46.9%
Minimum daytime 30-minute intensity	Q_{min}, *veh/interval*	516	543	622	+5.2%	+20.5%
Share of passenger cars, %	f_{car}	82.1	87.7	90.4	+5.6 p.p.	+8.3 p.p.
Share of trams, %	f_{tram}	5.70	4.73	4.21	−0.97 p.p.	−1.49 p.p.
Calculated indicators						
Daily variability coefficient	k_d	1.215	1.303	1.301	+7.3%	+7.1%
Peak hour factor	PHF	0.958	0.974	0.966	+1.6%	+0.9%
Coefficient of variation of total flow	CV	0.169	0.210	0.183	+24.3%	+7.9%
Peak asymmetry coefficient (evening/ morning)	k_{peak}	1.110	1.342	1.214	+20.9%	+9.4%
Saturation flow (veh. pcu/ interval)	$\bar{\mu}_{PCE}$	1115.1	1224.9	1375.8	+9.8%	+23.4%
Share of A in the total flow	f_A	29.3%	1.3%	15.2%	−28.0 p.p.	−14.1 p.p.
Share of B in the total flow	f_B	19.1%	43.6%	41.4%	+24.5 p.p.	+22.3 p.p.
VMR of the total flow	VMR	25.16	46.12	40.16	+83.3%	+59.6%
NBD aggregation parameter (approach B)	$\hat{r}_{NB}$ (B)	31.66	25.54	35.47	−19.3%	+12.1%
Maneuver entropy for approach A (normalized)	$\hat{H}_A$	0.393	0.039	0.497	−90.0%	+26.5%
P95 of the total flow (Gumbel)	P95, *veh/interval*	1322	1622	1835	+22.7%	+38.8%
P99 of the total flow (Gumbel)	P99, *veh/interval*	1609	2003	2244	+24.5%	+39.4%
Redistribution coefficient (approach B)	r_B	-	1.175	1.358	-	-
Hysteresis index (approach B), %	HHI_B	-	-	−197.7	-	-
Hysteresis index (approach A), %	HHI_A	-	-	+28.8	-	-

Note. PCU - passenger car unit equivalency factors assigned in accordance with HBS 2015 [21] guidelines (passenger car = 1.0; bus = 2.5; tram = 3.0; motorcycle = 0.5); p.p. - percentage points.

5 Design results and statistical interpretation

5.1 Stochastic dispersion structure and parameters of the negative binomial distribution

To better understand the microscopic nature of traffic flow redistribution, an analysis of the dispersion structure of empirical samples was conducted using the negative binomial distribution (NBD) model.

Table 2 presents the parameters of the negative binomial distribution and the results of the ANOVA analysis.

The behavior of direction A in S2 is particularly noteworthy: VMR = 0.330 < 1. Underdispersion is a rare phenomenon in traffic flows, indicating a nearly deterministic nature of the process.

The physical explanation is that the entire residual flow in direction A in S2 consists exclusively of trams operating according to a fixed schedule. This regime is better approximated not by Poisson or standard binomial models, but by a Neyman Type A distribution or a degenerate (deterministic) process. However, for short-term traffic flows characterized by high variance and clustered vehicle arrivals (often exacerbated by upstream signal influences or varying time resolutions) the negative binomial distribution remains a highly suitable and empirically validated choice, as demonstrated by Akinfala et al. [22].

The remaining vehicular directions and time periods exhibit persistent overdispersion with VMR ∈ [5.05; 23.66].

The aggregation parameter $\hat{r}_{NB}$ attains its minimum value for direction D in S2 ($\hat{r}$ = 17.94) - This indicates maximal clustering, reflecting the amplification of peak “waves” in this direction under congested conditions. The dispersion analysis yields η^2 = 0.912 for A and η^2 = 0.739 for B, the time-of-day factor explains

Table 2 NBD Parameters and ANOVA Results

Direction	Day	$\bar{\mu}$ (interval)	σ^2	VMR	$\hat{r}_{NB}$	$\hat{p}_{NB}$	*F* (ANOVA)	η^2
	S1	257.70	1301.8	5.052	63.61	0.198	212.9***	0.912
A	S2	14.00	4.62	0.330”	-	-		
	S3	183.41	1906.5	10.395	19.52	0.096		
	S1	167.50	1053.6	6.290	31.66	0.159	58.1***	0.739
B	S2	453.82	8516.4	18.766	25.54	0.053		
	S3	498.59	7507.3	15.057	35.47	0.066		
	S1	68.50	659.6	9.629	7.94	0.104	35.0***	0.631
C	S2	166.71	1307.9	7.845	24.35	0.128		
	S3	99.71	903.9	9.065	12.36	0.110		
	S1	384.50	4639.8	12.067	34.74	0.083	0.64*	0.030
D	S2	406.59	9621.6	23.664	17.94	0.042		
	S3	422.94	6512.6	15.398	29.37	0.065		

*Note. *** - p < 0.001; * - p > 0.05; “ - VMR < 1 (underdispersion; corresponds to the deterministic schedule of public transport).*

Table 3 Redistribution matrix of normalized flow intensities and comparison statistics

Direction	S1, $\bar{\mu}$ [95% CI]	S2, $\bar{\mu}$ [95% CI]	S3, $\bar{\mu}$ [95% CI]	Δ(S1→S2)	|d| Cohen	r_i
A	257.70 [231.9; 283.5]	14.00 [12.9; 15.1]	183.41 [161.0; 205.9]	−243.7***	9.54	-
B	167.50 [144.3; 190.7]	453.82 [406.4; 501.3]	498.59 [454.0; 543.1]	+286.3***	4.14	1.175
C	68.50 [50.1; 86.9]	166.71 [148.1; 185.3]	99.71 [84.2; 115.2]	+98.2***	3.13	0.403
D	384.50 [335.8; 433.2]	406.59 [356.2; 457.0]	422.94 [381.4; 464.4]	+22.1 n.s.	0.26	0.091

*Note. *** - p < 0.001 (the Welch's t-test).* $r_i = \Delta_i(S1 \rightarrow S2) / |\Delta_A|$; $\Sigma r_i = 1.66$ - overcompensation.

91% and 74% the total variance, respectively. For D $\eta^2 = 0.030$ ($F = 0.64$, $p = 0.533$): This direction is invariant with respect to the restriction regime and operates independently under saturated conditions.

5.2 Maneuver entropy and structural transformation

Shannon entropy in direction A exhibits a sharp degradation in S2 ($\hat{H}$: 0.393 → 0.039 → 0.497) and, importantly, an exceedance of the baseline level in S3. This behavior reflects genuine structural enrichment: after the restoration of operation in A, a portion of drivers returning via B→A increases the share of maneuver AB (straight) from 14.1% to 26.7%, thereby raising the entropy. The increase in $\hat{H}A$ from 0.393 to 0.497 (S1 → S3) constitutes a measurable routing footprint of hysteresis: the structure of maneuver choice does not fully revert even after the removal of the restriction.

For direction D, the entropy increases from S1 ($\hat{H} = 0.501$) to S2 ($\hat{H} = 0.738$) and remains stably elevated in S3 ($\hat{H} = 0.742$). The emergence of a significant D→A flow (right turn, p = 0.000 → 0.327) and the simultaneous reduction of D→C (straight-through, p = 0.362 → 0.147) form a new stable routing structure that persists after the repair-providing quantitative, entropy-based evidence of hysteresis, independent of mean flow intensities.

5.3 Redistribution matrix, r_i coefficients, and queue analysis

Table 3 presents the redistribution matrix with 95% confidence intervals (CI) and the results of the Welch's t-test.

The global balance of transport demand was assessed using a redistribution matrix, with 95% confidence intervals (95% CI) and application of the Welch's t-test. The blockage of the entry generated an absolute loss at approach A of ΔA = -243.7 units per time interval. However, the network compensation proved to be asymmetric. At the adjacent approach B, an increase was observed ΔB = +286.3 veh/interval, which corresponds to a redistribution coefficient of $r_B = 1.175$. Together with the increases in directions C ($r_C = 0.403$) and D ($r_D = 0.091$), the aggregate system index reached $\Sigma r_i = 166$.

A value of $\Sigma r_i > 1$ constitutes evidence of the activation of induced (latent) demand. The loss of capacity on the primary direction A triggered a macroscopic rerouting by drivers across the entire Leipzig network. Road users who had previously avoided Augustusplatz due to its consistently high load altered their trajectories, attracted by the released signal phases for directions B and C, thereby generating a paradoxical excess accumulation of traffic. This effect represents a local manifestation of mechanisms akin to the Braess paradox and the Downs-Thomson paradox, whereby a change in the capacity of a single network segment can disproportionately degrade the performance of the entire system.

The estimation of effect sizes using the standardized metric of Jacob Cohen indicates a substantial shift in the distributions: for direction A, $|d| = 9.54$, and for direction B, $|d| = 4.14$. These values exceed the conventional "large effect" threshold ($d \geq 0.80$) by an order of magnitude, indicating that the statistical distributions of flow intensities in Scenarios 1 and 2 are practically non-overlapping.

5.4 Microscopic delay modelling and the spillback effect in oversaturated states (M/G/1)

For a quantitative assessment of the viability of the existing traffic signal control plans, an approximation based on queueing theory for an M/G/1 system was employed. In S2, the system crossed the boundary of phase stability: all the three active vehicular channels operated in an oversaturated regime with utilization factors $\rho > 1$ ($\rho_B = 1.261$; $\rho_C = 1.235$; $\rho_D = 1.506$).

In S3 (after the removal of restrictions), directions B and D failed to return to a stable state. ($\rho_B = 1.385$; $\rho_D = 1.566$). By contrast, approach C stabilized ($\rho_C = 0.739$). Using the Pollaczek-Khinchine formula for direction C, the expected queue length under steady-state conditions was $L_q \approx 1.6$ veh, while the mean waiting delay was $W_q \approx 28.3$ s.

However, for directions with $\rho > 1$, the stationary model breaks down. Let us model the development of congestion for approach B in S3 ($\lambda = 498.6$ veh/interval, $\mu_c = 360$ veh/interval). The deficit accumulation rate is $\Delta q = \lambda - \mu_c \approx 138$ vehicles per half-hour. With an average dynamic vehicle length of $l_v = 6.5$ m, such a queue requires nearly 900 m of storage space. Given that the distance to the nearest arterial intersection is approximately 250 m, corresponding to a storage capacity of $N_{max} \approx 38$ vehicles per lane, the time to full upstream blocking of the adjacent node, i.e., the spillback effect, is calculated as:

$$t_{spill} = \frac{N_{\max}}{\Delta q} \cdot 30 = \frac{38}{138} \cdot 30 \approx 8.2\,\text{minutes}. \tag{17}$$

Thus, the current signal timing plan, optimized for the baseline conditions of S1, is suboptimal for the modified routing matrices of S2 and S3. Without the reallocation of green phase durations, the junction generates network-wide breakdowns every 8-10 minutes under peak demand conditions.

5.5 Spatial concentration and structural transformation of traffic flows: Herfindahl-Hirschman Index (HHI) analysis

To quantitatively assess the spatial redistribution of traffic load across directions, the Herfindahl-Hirschman Index (HHI), adapted to the transportation context, was employed:

$$HHI = \sum_i p_i^2, \tag{18}$$

where:

p_i is the share of the i-th direction in the total intersection flow. A value of HHI→1 corresponds to extreme concentration of traffic on a single direction, whereas HHI→1/n indicates a uniform distribution across n directions.

The HHI calculation results are presented in Table 1. Under S3, the HHI_A index increased by +28.8% relative to the normal level, indicating a pronounced concentration of flow toward approach A, which had previously been blocked. In contrast, HHI_B exhibited a sharp decline of −197.7%: this abrupt "dispersion" of traffic reflects disorientation in route choice under conditions of complete removal of dominant inflow/outflow paths. Notably, even after full stabilization of the junction operation, none of the indices returned to their baseline values. This is consistent with the results of the entropy-based analysis (Section 5.2) and constitutes the structural evidence of route hysteresis: the system "retains" the deformed distribution matrix and maintains it even after all constraints have been fully lifted.

Complementing the spatial dimension, a temporal analysis of diurnal variability was performed. The peak hour factor (PHF) increased from 0.958 in S1 to 0.974 in S2, indicating a smoothing of micro-peak fluctuations and a transition of the flow toward a quasi-stationary oversaturated state. The daily variability coefficient rose from 1.215 to 1.303, suggesting that, in an effort to avoid congestion during the conventional morning peak, drivers shifted their trips, thereby extending the temporal distribution of demand. The evening peak gained absolute dominance over the morning peak: the peak ratio index k_{peak} increased from 1.11 to 1.342, reflecting an altered rhythm of commuting patterns under perturbed conditions.

The HHI and the temporal coefficients are complementary indicators of the same process: an infrastructure perturbation deforms the transport system simultaneously in space (concentration/dispersion across directions) and in time (shifts and smoothing of the peak demand profile).

6 Conclusions

The conducted study made it possible to mathematically formalize the patterns of spatiotemporal redistribution of traffic flows under infrastructure-induced disturbances and to develop a toolkit for proactive management of the urban road network. Based on the results of the field quasi-experiment at Augustusplatz and the application of a set of stochastic models, the following key conclusions were obtained:

1. **Stochastic heterogeneity and rejection of the Poisson paradigm.** It has been demonstrated that under conditions of roadway capacity reduction, the traffic flow loses the properties of random arrivals. High clustering of passenger cars leads to pronounced overdispersion (VMR >> 1), which necessitates the use of the negative binomial distribution (NBD) for accurate queue modelling. At the same time, isolated scheduled transport (trams) exhibits underdispersion (VMR = 0.33), forming a stable deterministic component within an oversaturated system.
2. **Asymmetry of network response and induced demand.** The nonlinear nature of macroscopic effects depending on the topology of restrictions has been established. Blocking the downstream channel triggers an overcompensation effect: the attraction of latent (induced) demand leads to a situation where the total increase in traffic on adjacent directions significantly exceeds the blocked volume ($\sum r_i = 1.66$). This locally degrades system performance due to mechanisms akin to the Braess paradox. In contrast, upstream closure is accompanied by macroscopic "traffic evaporation."
3. **Indicators of route hysteresis.** Using Shannon entropy ($\hat{H}$) and standardized effect sizes (Welch's *t*-test, Cohen's *d*), the potential presence of transport network inertia has been outlined. The data suggests that the system does not immediately return to its initial equilibrium state after the complete removal of restrictions. A residual structural deformation of the maneuver matrix is observed, accompanied by an increase in entropy ($\Delta\hat{H} > 0$), which may indicate a temporary or long-term shift in drivers' cognitive perception of detour routes.
4. **Phase transitions and the spillback effect.** The M/G/1 queueing approximation verified the transition of the system into an unstable (oversaturated) state ($\rho > 1$) during peak loads. The calculations show that maintaining baseline signal timing plans under conditions of induced demand can generate upstream blocking of adjacent intersections (spillback) as early as the eighth minute of the oversaturation phase, triggering a cascading degradation of network capacity.
5. **Study limitations**. The empirical framework is constrained by the recording of a single observation day per scenario over different months of 2025. As a result, the observed differences between scenarios may partially encompass underlying day-to-day or seasonal demand volatility, weather impacts, or specific network conditions of those days. Future research should aim to collect multi-day samples to rigorously control for temporal autocorrelation and further isolate the pure effects of channel closures.

Acknowledgements

This publication was issued thanks to supporting the Cultural and Educational Grant Agency of the Ministry of Education of the Slovak Republic in the projects No. KEGA 024ZU-4/2024: Deepening the knowledge of university students in the field of construction of transport means by carrying out professional and scientific research activities in the field, No. KEGA 024ZU-4/2025: Enhancing the knowledge of engineering students on progressive methods of maintenance and diagnostics of vehicles.

Conflicts of interest

The authors declare that they have no known competing financial interests or personal relationships that could have appeared to influence the work reported in this paper.

References

[1] KRAVCHENKO, O., KHRULEV, A., GERLICI, J., SARAIEV, O., DANETS, S. Technical condition assessment and modelling of reed valves in vehicle engine intake systems. *Communications - Scientific Letters of the University of Zilina* [online]. 2025, **27**(1), p. B41-B52. ISSN 1335-4205, eISSN 2585-7878. Available from: https://doi:10.26552/com.C.2025.006

[2] KRAVCHENKO, O., SYMONENKO, R., GERLICI, J., GOLOVAN, A., SHYMANSKYI, S., GRITSUK, I., and GRYTSUK, Y. Research on the use of biogas as an additive to compressed natural gas for supplying vehicle engines. *Communications - Scientific Letters of the University of Zilina* [online]. 2025, **27**(3), p. B158-B169. ISSN 1335-4205, eISSN 2585-7878. Available from: https://doi:10.26552/com.C.2025.034

[3] WEBSTER, F. V. Traffic signal settings. Road research technical paper no. 39. London: HMSO, 1958.

[4] AKCELIK, R. Traffic signals: capacity and timing analysis. ARRB research report ARR no. 123. Vermont South: ARRB, 1981.

[5] NEWELL, G. F. Queues for a fixed-cycle traffic light. *The Annals of Mathematical Statistics* [online]. 1960, **31**(3), p. 589-597. ISSN 0003-4851, eISSN 2168-8990. Available from: https://www.jstor.org/stable/2237570
[6] LORD, D., MANNERING, F. The statistical analysis of crash-frequency data: a review and assessment of methodological alternatives. *Transportation Research, Part A* [online]. 2010, **44**(5), p. 291-305. ISSN 0965-8564, eISSN 1879-2375. Available from: https://doi.org/10.1016/j.tra.2010.02.001
[7] ELVIK, R. The predictive validity of empirical Bayes estimates of road safety. *Accident Analysis and Prevention* [online]. 2008, **40**(6), p. 1964-1969. ISSN 0001-4575, eISSN 1879-2057. Available from: https://doi.org/10.1016/j.aap.2008.07.007
[8] HAUER, E. Overdispersion in modelling accidents on road sections and in empirical Bayes estimation. *Accident Analysis and Prevention* [online]. 2001, **33**(6), p. 799-808. ISSN 0001-4575, eISSN 1879-2057. Available from: https://doi.org/10.1016/S0001-4575(00)00094-4
[9] ZHANG, S., AN, H. K., YUEN, C. W. A Study on traffic flow distribution in road networks considering the impact of construction zones. *Promet - Traffic and Transportation* [online]. 2025, **37**(5), p. 1354-1375. ISSN 0353-5320, eISSN 1848-4069. Available from: https://doi.org/10.7307/ptt.v37i5.860
[10] ADLER, M. W., VAN OMMEREN, J. N. Does public transit reduce car travel externalities? Quasi-natural experiments' evidence from transit strikes. *Journal of Urban Economics* [online]. 2016, **92**, p. 106-119. ISSN 0094-1190, eISSN 1095-9068. Available from: https://doi.org/10.1016/j.jue.2016.01.001
[11] WILSON, A. G. *Entropy in urban and regional modelling*. London: Pion, 1970. ISBN 9780415696319.
[12] LIN, J., BAN, Y. Complex network topology of transportation systems. *Transport Reviews* [online]. 2013, **33**(6), p. 658-685. ISSN 0144-1647, eISSN 1464-5327. Available from: https://doi.org/10.1080/01441647.2013.848955
[13] FILIPOVSKA, M., MAHMASSANI, H., MITTAL, A. Estimation of path travel time distributions in stochastic time-varying networks with correlations. *Transportation Research Record: Journal of the Transportation Research Board* [online]. 2021, **2675**(11), p. 498-508. ISSN 0361-1981, eISSN 2169-4052. Available from: https://doi.org/10.1177/036119812110184
[14] KINGMAN, J. F. C. The single server queue in heavy traffic. *Mathematical Proceedings of the Cambridge Philosophical Society* [online]. 1961, **57**(4), p. 902-904. ISSN 0305-0041, eISSN 1469-8064. Available from: https://doi.org/10.1017/S0305004100036094
[15] GUPTA, G. K. Traffic signal control using {M/G/1/N} queue: new results. *International Journal of Mathematics and Computer Science* [online]. 2025, **20**(3), p. 877-880. ISSN 1814-0424, eISSN 1814-0432. Available from: https://doi.org/10.69793/ijmcs/03.2025/gupta
[16] SOKHATSKYI, A. V., LESNIKOVA, I. Y., TROFIMOV, O. V., KHALIPOVA, N. V., KUZMENKO, A. I. *Modelling in transport technologies. Part I.* Dnipro: University of Customs and Finance (UMSF), 2022. ISBN 978-966-328-191-9.
[17] FORNALCHYK, Y. Y., HILEVYCH, V. V., MOHYLA, I. A. Traffic flow modelling: Lviv: Lviv Polytechnic Publishing House, 2020. ISBN 978-966-941-417-5.
[18] STEPANCHUK, O. V., REITSEN, Y. O., BELIATYNSKYI, A. O. Modelling of traffic flows on urban road networks. *Proceedings of National Aviation University*, 2014, **2**(3), p. 10-29. ISSN 1813-1166, eISSN 2306-1472.
[19] KIRKIN, O. P., KIRKINA, V. I., KIRKINA, T. Y. New analytical methods for traffic flow management based on system studies in logistics. *Bulletin of Pryazovsky State Technical University. Series: Engineering Sciences.* 2017, **34**, p. 209-216. ISSN 2225-6733, eISSN 519-271X.
[20] UKRAINSKYI, Y. O., UKRAINSKA, T. A., HANZHEIEV, D. I. Prospects for the development of operational traffic flow management methods under urban road network conditions. *Scientific Notes of Taurida National V. I. Vernadsky University. Series: Engineering Sciences*. 2020, **31**(70), p. 234-238. ISSN 2663-5941, eISSN 2663-595X.
[21] Road and Transportation Research Association. HBS 2015: Manual for the capacity analysis of highways and streets. Cologne: FGSV Verlag, 2015.
[22] AKINFALA, O. O., EGE, E. E., OGUNWOLU, L. F. Arrival patterns and traffic flow characteristics at signalized intersections: considering upstream signal influence and time resolutions. *FUTA Journal of Engineering and Engineering Technology* [online]. 2021, **15**(1), p. 11-28. ISSN 1598-0271, eISSN 2636-6045. Available from: https://doi.org/10.51459/futajeet.2021.15.1.208